

## Article

# Critical Tectonic Limits for Geothermal Aquifer Use: Case Study from the East Slovakian Basin Rim

Stanislav Jacko \*, Roman Farkašovský, Igor Ďuriška, Barbora Ščerbáková and Kristína Bátorová

Institute of Geosciences, Faculty BERG, Technical University of Košice, 04001 Košice, Slovakia; roman.farkasovsky@tuke.sk (R.F.); igor.duriska@tuke.sk (I.Ď.); barbora.scerbakova@tuke.sk (B.Š.); batorova.kristina@gmail.com (K.B.)

\* Correspondence: stanislav.jacko@tuke.sk; Tel.: +42-155-602-31-35

**Abstract:** The Pannonian basin is a major geothermal heat system in Central Europe. Its peripheral basin, the East Slovakian basin, is an example of a geothermal structure with a linear, directed heat flow ranging from 90 to 100 mW/m<sup>2</sup> from west to east. However, the use of the geothermal source is limited by several critical tectono-geologic factors: (a) Tectonics, and the associated disintegration of the aquifer block by multiple deformations during the pre-Paleogene, mainly Miocene, period. The main discontinuities of NW-SE and N-S direction negatively affect the permeability of the aquifer environment. For utilization, minor NE-SW dilatation open fractures are important, which have been developed by sinistral transtension on N-S faults and accelerated normal movements to the southeast. (b) Hydrogeologically, the geothermal structure is accommodated by three water types, namely, Na-HCO<sub>3</sub> with 10.9 g·L<sup>-1</sup> mineralization (in the north), the Ca-Mg-HCO<sub>3</sub> with 0.5–4.5 g·L<sup>-1</sup> mineralization (in the west), and Na-Cl water type containing 26.8–33.4 g·L<sup>-1</sup> mineralization (in the southwest). The chemical composition of the water is influenced by the Middle Triassic dolomite aquifer, as well as by infiltration of saline solutions and meteoric waters along with open fractures/faults. (c) Geothermally anomalous heat flow of 123–129 °C with 170 L/s total flow near the Slanské vchy volcanic chain seems to be the perspective for heat production.

**Keywords:** geotherm; heat flow; permeability; structural modeling; seismic; resources; renewable; utilization; Pannonian basin; East Slovakian basin



**Citation:** Jacko, S.; Farkašovský, R.; Ďuriška, I.; Ščerbáková, B.; Bátorová, K. Critical Tectonic Limits for Geothermal Aquifer Use: Case Study from the East Slovakian Basin Rim. *Resources* **2021**, *10*, 31. <https://doi.org/10.3390/resources10040031>

Academic Editor: Michela Costa

Received: 2 March 2021

Accepted: 31 March 2021

Published: 2 April 2021

**Publisher's Note:** MDPI stays neutral with regard to jurisdictional claims in published maps and institutional affiliations.



**Copyright:** © 2021 by the authors. Licensee MDPI, Basel, Switzerland. This article is an open access article distributed under the terms and conditions of the Creative Commons Attribution (CC BY) license (<https://creativecommons.org/licenses/by/4.0/>).

## 1. Introduction

Geothermal energy represents a very attractive, economic, and ecologic energy source. The utilization of geothermal energy for commercial purposes, which is mainly a result of the increase of world fuel prices, as well as new technologies, proved to be an essential action for the realization of programs benefiting from this heat source. The necessity of the use of renewable energy resources (including geothermal energy) in Slovakia stems from both international trends, above all the countries of European communities, and from the increase of fuel prices on the world markets. The increased interest in renewable resources stems from the high priority in the human environment. All these factors caused that the topic of renewable energy is an important agenda not only for scientists, but also for politicians and business activities. As the socio-political pressure increases towards the transition to low global carbon and sustainable future, the role of geothermal energy usage worldwide intensifies [1]. In 2020, there are records quantified records of direct geothermal utilization worldwide in 88 countries [2]. This is an increase in direct utilization from 82 countries reported in 2015 [3], 78 countries reported in 2010 [4], 72 countries reported in 2005 [5], and 58 countries reported in the year 2000 [6]. Around 283.58 Terawatt-hours (TWh) of geothermal heat are being used worldwide each year. An estimation of the worldwide installed thermal power at the end of 2019 is 107.7 GW which is a 52% increase from 2015. Moreover, the thermal energy used increased from 2015 by 72.3% to 1,020,887 TJ/year [2]. The distribution of the used geothermal energy used by category is

approximately 58.8% for ground-source heat pumps, 18.0% for bathing and swimming, 16.0% for space heating (of which 91.0 % is for district heating), 3.5% for greenhouse and open ground heating, 1.6% for industrial process heating, 1.3% for aquaculture pond and raceway heating, 0.4% for agricultural drying, 0.2% for snow melting and cooling, and 0.2% for other applications (desalination, bottle washing, animal farming, etc.) [7]. For the last five years, the number of wells drilled was 2647; the combined effort of professionals working on geothermal energy was 34,500 person-years, and the total worth invested into projects was 22.262 billion US\$ [2]. The production cost for geothermal heating is highly variable. The cost is highly dependent on the quality of the geothermal resource and the investment needed for recovery, especially the number and depth of wells required and the distance from the wells to the point of use. Geothermal heat could be transported over a considerable distance from the source to consumers. The longest single geothermal hot water pipeline in the world is located in Iceland (62 km) [8].

The Pannonian basin is one of the most significant geological structures in Central Europe. The basin evolution is related to thermal impact when crustal fragments have been directly subjected to crustal melting in the Carpathian embayment [9]. Heat flow distribution in the Pannnoanian basin shows values ranging from 50 to 130 mW/m<sup>2</sup> [9–12]. The average heat flow is considerably higher in the Great Hungarian Plain, than in the Carpathians. Especially in the East Slovakian basin [13–15] are heat flow values above 100 mW/m<sup>2</sup> (Figure 1).

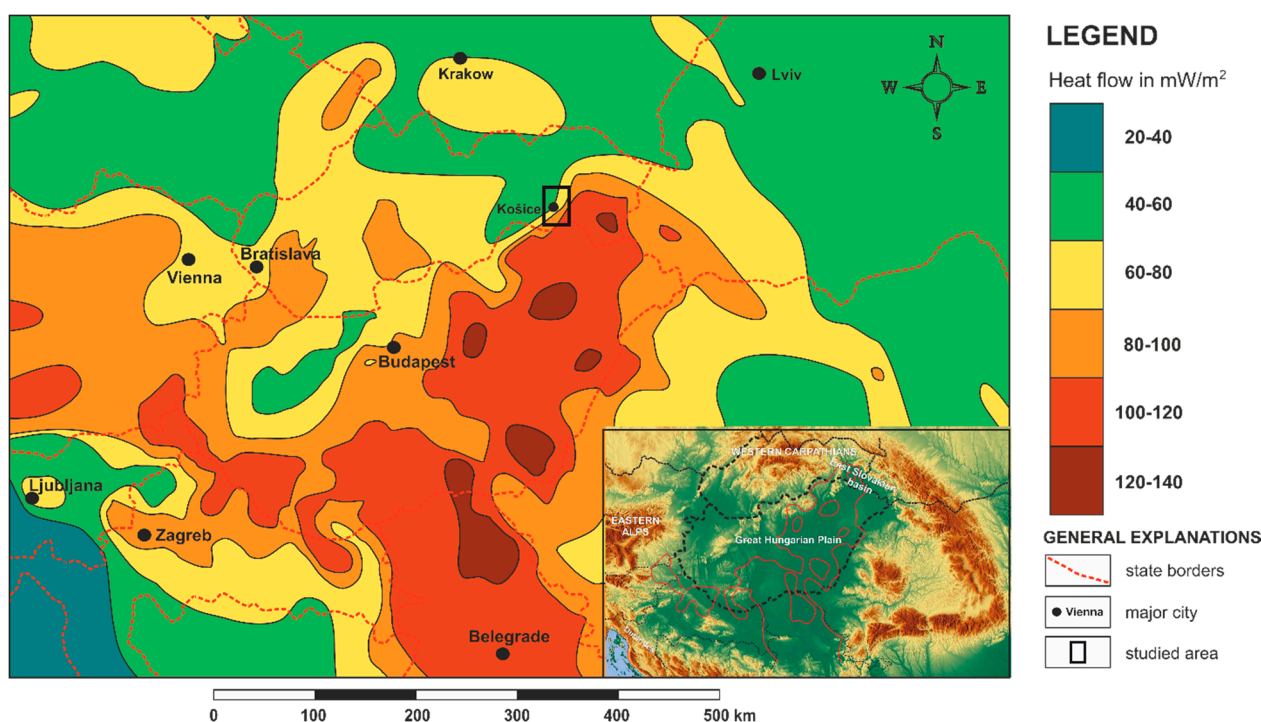


**Figure 1.** The heat flow distribution in the Pannonian basin and their peripheral areas (values in mW/m<sup>2</sup>). The East Slovakian basin is an integral part of the major heat flow system in Central Europe (modified after [9,10]).

The East Slovakian Basin is part of the extensive Pannonian basin that formed during the Miocene. The basin is divided by the Slanské vrchy neovolcanic chain into the eastern, i.e., the Trebišov depression, and the western, the Košice depression. The Košice depression is the area with the highest potential for geothermal use, including the generation of electricity in Slovakia. In general, geothermal sources in the Slovakia territory and their utilization are influenced by two “unknown” basic parameters: Geothermal fluids and temperature.

The main sources of geothermal water in the Western Carpathians are usually linked with the Middle-Upper Triassic dolomites. Geological processes during the closure of

the Carpathian orogeny uplifted [16], and eroded the overlying sedimentary rocks of the Upper Triassic to Cretaceous age. They were eroded to the dolomite level. Subsequent karstification of the dolomites created the ideal aquifer in the region. The heat flow is related to the evolution of the Pannonian basin [17–19]. During the Miocene, basin subsidence accelerated, due to the ascent of asthenolite. The result was earth crust thinning, rifting, as well as the formation of the peripheral basins [20], at the northern edge of the Pannonian basin. These individualized sedimentary basins are considered the most important and the most suitable geothermal areas in Slovakia with a relatively high heat flow. Geothermal water in the wells was found at depths ranging from 92 m to 3616 m. Free outflow in the wells ranged from 0.1 up to 100 l/s. Na-HCO<sub>3</sub>-Cl, Ca-Mg-HCO<sub>3</sub>, and Na-Cl chemical type of waters with the TDS value of 0.4–90.0 g·L<sup>-1</sup> prevail. The temperatures vary from 20 to 74 °C in 1000 m depth, with an average value of 45 °C. Overall in Slovakia 230.3 MW and 2000.9 TJ/year are utilized [21]. Geothermal energy for heating is registered in 68 localities (Figure 2a), 39 localities are useable for swimming and bathing, 11 for drying, 6 for commercial use, 4 localities for district heating, and only one locality for fish farming.

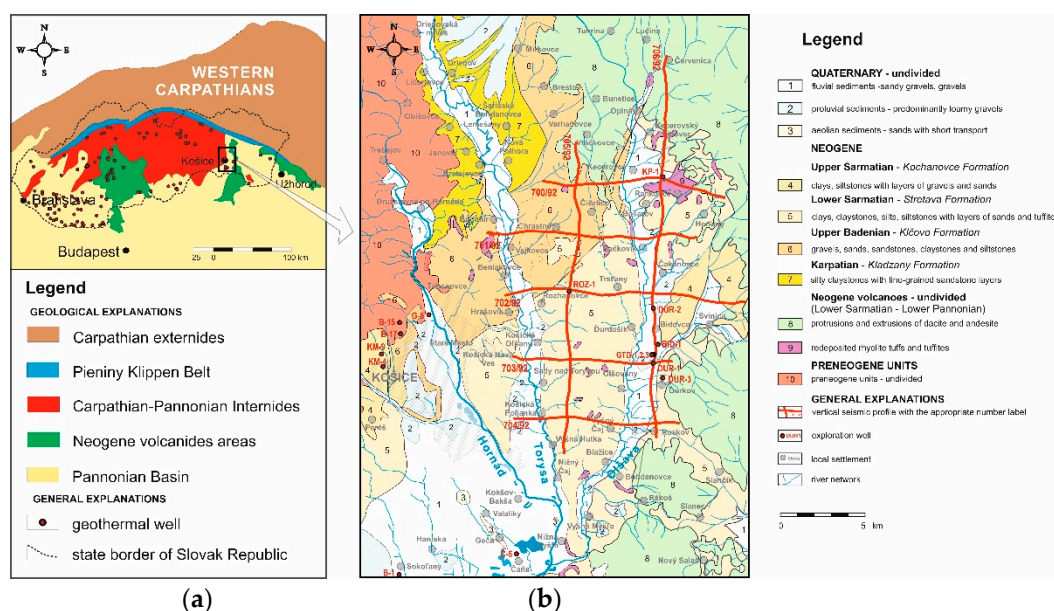


**Figure 2.** Simplified geological maps (a) Utilization of the geothermal sources in Slovakia is localized mainly on the west side of the territory. Producing wells are situated in the same aquifer as in the Košice depression. (b) Košice depression lies in the west part of the East Slovakian basin. In the geological map are important wells and deep 2D seismic cross-sections localization use in the article faults (modified after [21–23]).

The article aims to analyze additional parameters, such as tectono-geological limits in the potential geothermal area. The processes of multiple deformations that modified tectonic and sedimentary structures, had a limiting effect on aquifer spatial distribution, the chemistry of fluids (open dislocations), hydraulic parameters (subsidence/uplift), the temperature (thermolift), lithology and wells construction. Parameters of each thermal resource have an impact on total initial cost and confirmation of economic and technical feasibility.

## 2. Materials and Methods

The data set consisted of several types of technical data, which were used to create a structural model and a 3D model of the aquifers. The 3D model of the southeastern part of the Kosice basin displays a spatial distribution of the aquifers and overlying Neogene insulators and spatial thickness transition of the aquifers and their relations to tectonic structures. Data processing [24], correlation of 2D seismic profiles vs. well data, and interpretation (Figure 3) have been realized in the Petrel software. The modeling workflow

includes depth conversion, establishing horizons, volume calculation, and geometrical modeling. Data from the wells that were used in the model can be divided into three groups [25–27]. The first group of wells: Structural KP-1, DUR-1, DUR -2, ROZ-1, and geothermal key wells, GTD-1, GTD-2, and GTD-3, are situated in the Košice depression. The second group of wells: Kosice KM-4, Kosice G5, Kosice KM-9, Drienov-2, Bankov-15, Bankov-17 are localized at the west edge of the Košice depression. The third group of wells is situated in the south Gemeric unit. They are without carbonates and dolomites in the subsurface: Bociar-1, Cana-6, Komarovce-1. Structural and lithostratigraphic interpretations come out from 2D seismic cross-sections No. 700/92, 702/92, 703/92, 704/92, 705/92, and 706/92 (Figures 2b and 4). Based on these results, it was possible to distinguish five following reliably indicative lithostratigraphic interfaces. They separate rock complexes of the different evolution stages of the area:

1. the basal plane of Mesozoic sequences
2. the interface of Mesozoic top/Karpatian formations
3. the interface between Karpathian/Early-Middle Badenian formations
4. Early-Middle Badenian/Late Badenian formations boundary
5. Late Badenian/Sarmatian formations boundary

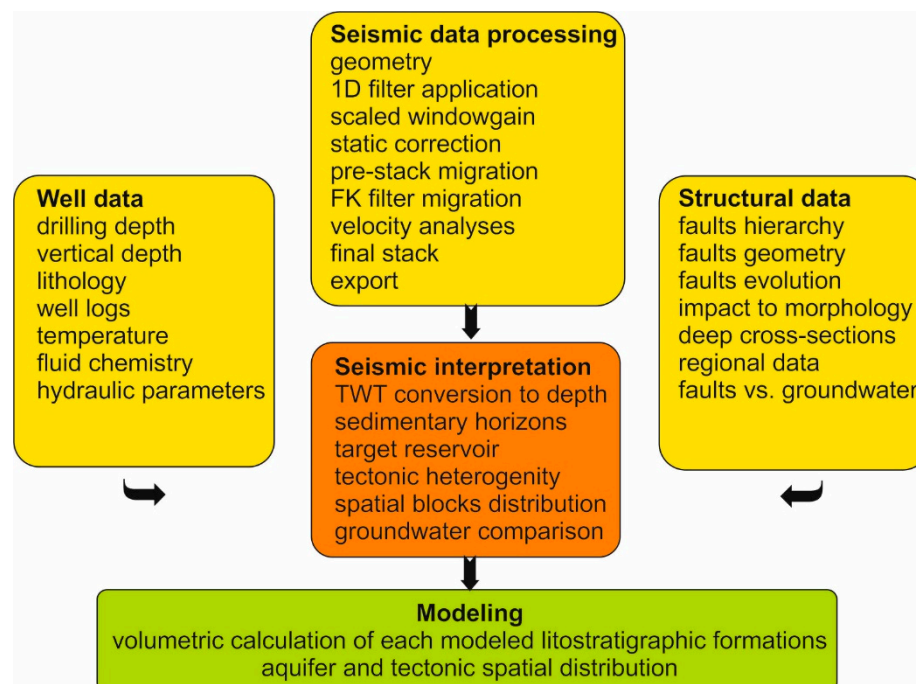


**Figure 3.** Integrated workflow diagram divided into three groups: Data collection (yellow), interpretation (orange), and modeling (green).

Fault interpretations do not fall into the important tasks of geological modeling. At this point, we have to emphasize that available seismic data belongs to 2D and not to a 3D category, i.e., they provide only limited possibilities for precise 3D modeling. The problem is moreover caused by relatively large (ca., 5–7 km) distances between the 2D seismic profiles. Individual faults could change their length, depth, and direction in the profile, or they could completely disappear, and new faults could emerge. For the above-mentioned reasons, the final 3D tectonic model presents a simplified structure of a lesser section of the area only. Due to the insufficient seismic data quality, fault tectonics is not included in the rest of the area. The 3D grid processed at the mentioned principles is ready for final 3D model elaboration and following interpretation steps. For the more precise demonstration of spatial distribution and changes in the thickness of the model's interior geostructural components, the model is sliced.



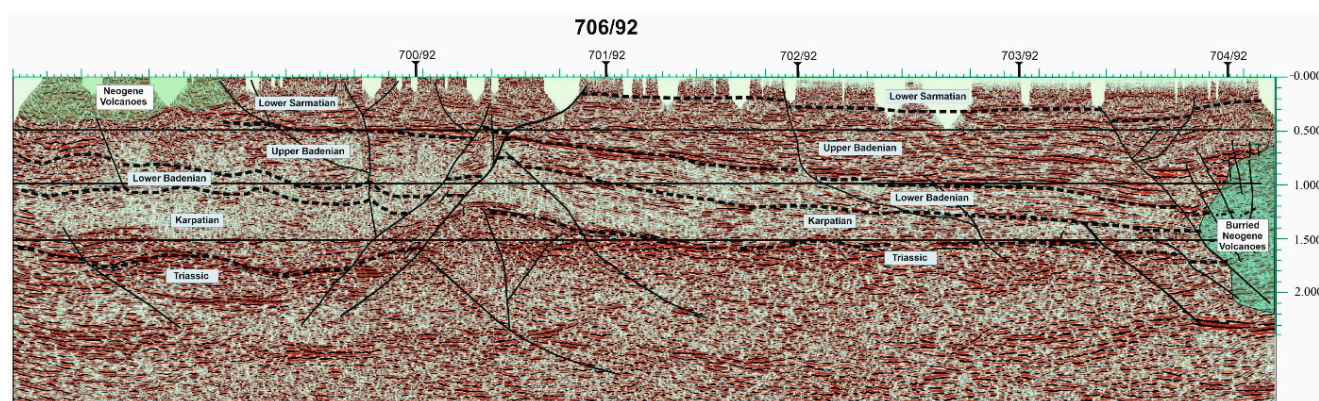


**Figure 4.** Deep seismic cross-section no. 706/92 oriented in a north–south direction. In the section are interpreted basic sedimentary formations and andesite volcanic rocks. A significant antiform (approximately in the middle part) represents the structural boundary between Čizatice and Durkov depressions. They are tectonically limited by NE–SW trending normal faults (modified after [28]).

### 3. Results

#### 3.1. Geology and Hydrogeological Conditions

The East Slovakian basin is filled by Karpatian/Pannonian volcano-sedimentary formations and Quaternary deposits (Figure 5). They substantially differ in their basement nature which has a direct consequence on hydrogeologic conditions of the depressions [29]. The base of the Košice depression Neogene formations exclusively comprises the Inner West Carpathian rock complexes. The footwall of its northern, i.e., the Prešov part, is formed by Paleogene sandstone/shale formations. Pre-Tertiary rock sequences of the Čierna hora Mts. (mainly Triassic dolomites and Paleozoic cover/crystalline complexes) are elevated at the western margin of the depression [30]. They submerge below the larger part of the Neogene fill of the depression. Especially a thick dolomite layer possesses very good conditions for water infiltration and groundwater circulation. Paleozoic rock complexes (mostly phyllites) of the Gemeric unit [31] form the main part of the depression footwall on the southwest. Their low water-saturation capacity is largely restricted to surface joints and weathering zone. The Triassic carbonates of the Čierna hora Mts. Underlying the depression on the western border are located at the geothermally less perspective area. Following actual exploration, the most promising part for the economic utilization of geothermal energy seems to be the southeastern part of the depression. In this area, 20 km distant eastward of Košice town, is the most potential Čizatice/Durkov area, where three positive geothermal wells, GTD-1, GTD-2, and GTD-3, have been drilled. The wells transected reservoir rocks (e.g., the Čierna hora Mts. Triassic dolomites) at 2850–3150 m depths. At the GTD-1 well, the water temperature reached 125 °C having 56 L·s<sup>−1</sup> discharge overflow. The water mineralization didn't exceed 30 g·L<sup>−1</sup> containing 96% of CO<sub>2</sub>. The water of the GTD-2 well, located westwardly from the previous one, achieved 124 °C and the discharge of 70 L·s<sup>−1</sup>. The mineralization doesn't exceed 28 g·L<sup>−1</sup> and 98% CO<sub>2</sub> content. The water of the geothermal well GTD-3 has reached 126 °C temperature and 150 L·s<sup>−1</sup> discharge.

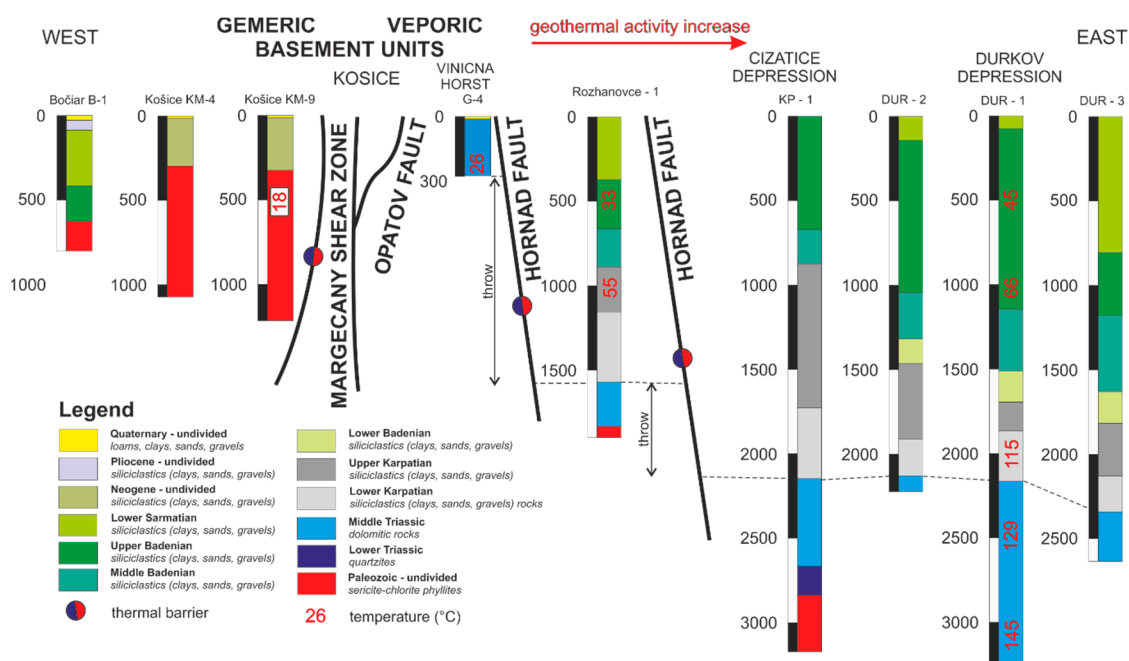


**Figure 5.** Structural deep wells with representative lithology and stratigraphy log in the Košice Depression. The wells are arranged from west to east. In the same direction, geothermal activity increase, and the dolomite aquifer rapidly drops down from the surface (0 m) to a depth of 2000 m. The aquifer is disintegrated into tectonic blocks on the Miocene/Quaternary Hornád fault system of N–S direction with normal fault activity (modified after [32–34]).

### 3.2. Structural Model

The spatial and depth extent of the geothermal aquifer in the Košice Basin is limited by the tectonic structure. The basin structure was developed by multiple deformations (Figure 6) of the basement underlier and sedimentary filling of the Neogene basin.

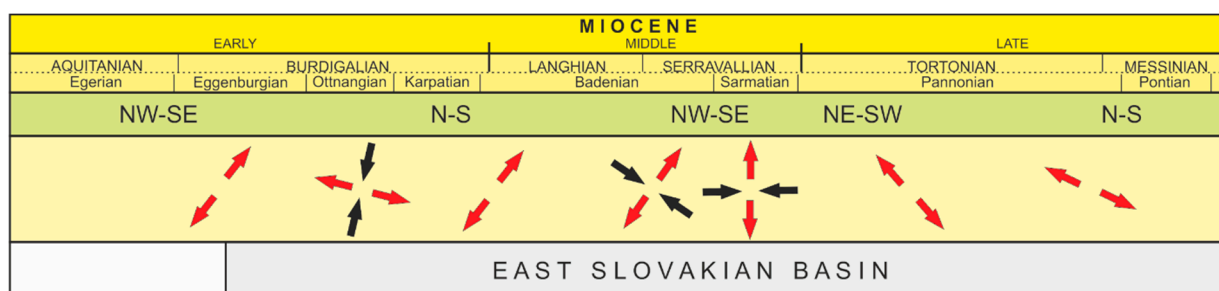


**Figure 6.** Paleostress orientation (red/tension; black/compression arrows) during the East Slovakian basin evolution. Deformation phases activate fault sets with one major system (green row). Distinct tectonic control is visible on seismic profiles, well cores, and outcrops. Their impact on basin basement, subsidence, and present morphology is significant (modified after [35]).

As a result of these processes, the aquifer is divided into segments, which run from the west to the east, creating a system of individual structural blocks with different vertical depositional depths (Figure 7). At the same time, individual measurements also show different permeability of the fault system, which affects the flow of thermal groundwater. In the Košice Depression, we can localize three differently oriented fault systems NW–SE, N–S, and NE–SW, which differ in age of origin, their activity, impact on the main dolomite geothermal aquifer, and impact on underlier morphology.

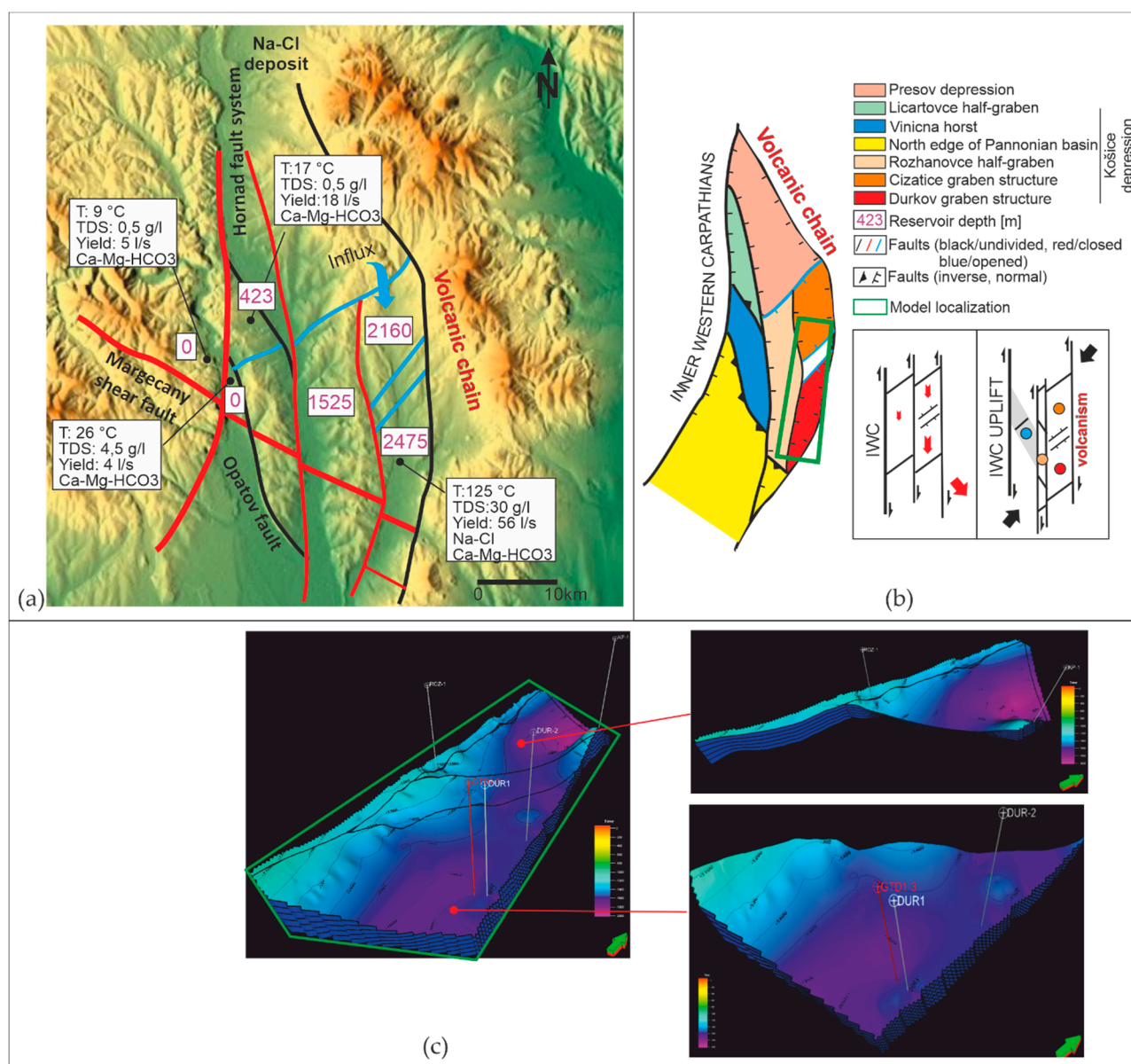


**Figure 7.** Block structure distribution bounded by three basic systems of NW–SE, N–S, and NE–SW directed faults in the territory of the Košice depression. (a) Interaction between morphology and tectonics is largely influenced by Miocene/Quaternary tectonics. The depth of the aquifer gradually increases from west to east to a depth of 2475 m at a distance of 20 km. (b) Sketch of two important deformation stages of tectonic structure development. The period of Upper Badenian was characterized by the delimitation of crust and its disintegration on N–S trending faults, while their asymmetric subsidence caused the formation of sinistral dips with subsequent formation of individualized shear basins. The Miocene uplift of the Inner Western Carpathians (IWC) was compensated at the edge with the East Slovakian basin by forming asymmetric shear bends, while externally from this zone, this uplift was compensated by oblique drops on the SE. (c) Block models of the Middle Triassic dolomites underlying the Košice Basin indicate significant irregularity and very significant tectonic limitation. Tectonic boundaries have different properties from the viewpoint of permeability (modified after [23]).

NW–SE fault system is parallel with the direction of major tectonic units of the Western Carpathians. Margecany shear zone is a pre-Mesozoic tectonic structure that tectonically divides the Gemeric unit (phyllites/low permeability) and the Veporic unit (dolomites/high permeability). The morphology and the fault rocks of the zone are on the surface best visible between the Košice and the Margecany towns. The activity of the zone has polystage character and was formed during the Alpine Cretaceous North–South



shortening of the Central Western Carpathians. The zone was reactivated several times during the Cretaceous-Neogene period. The zone is tens of meters wide on the surface. Towards the depth, the zone is lesser inclined to a subhorizontal position. Shear zone segments rocks of the crystalline complexes, as well as the rocks of the cover formations. Typical fault rocks are mylonites of the crystalline gneisses, mylonites of the Carboniferous and Permian meta-sediments, and mylonites of the Triassic quartzites. Mylonites have strong foliation and penetrative subhorizontal stretching lineation of the NW–SE direction. There are also occurring rauwackes of the Mesozoic carbonates. Therefore, this zone is the so-called “main limiting parameter”, which tectonically delimits the potentially usable area from the south. Parallel with this shear zone, the dislocations of the lower level were developed. Their multi-deformation history points out the structural diversity depending on paleo-stress conditions. The sigmoidal transpress bend of the Vinicna horst was developed at these fractures. Positive structures and local declines compensate the Miocene subsidence of the basin, e.g., subsidence of the Košice depression, rating from –285 m to –310 m during the post-Middle Miocene to Holocene period [29].

The N-S trending Hornád fault zone controls geomorphology of the depression. During the Paleogene/Quaternary period, the faults of the zone divided the Košice depression into individual sub-depressions with huge tectonic subsiding from west to east. Mostly eastwards (60–85°) inclined faults, forming 3 to 5 km wide zone, practically check the shape and filling of the depression, including geothermal carbonate reservoir and their underlying rock complexes. A relatively massive normal faulting represented a total rate of subsidence 2100 m at a distance of 20 km. The faults substantially influence the current submersion depth of these initially slowly eastwards inclined Miocene also formations. The polystage history of the fault is closely related to ESB opening during the Miocene period. According to structural research, it is possible to track deformation stages on the fault.

Huge subsidence of the ESB during the Early Miocene created a system of N–S depressions. Middle Miocene core delamination had an impact on the fault too. Asymmetric subsidence and plate rotation effect [36,37] caused sinistral shear movements with high intensity at the west ESB rim [38]. The basin breakdown is possible to correlate with horizons in the seismic cross-sections (Figures 4 and 5) and with subdivision into blocks, horsts, and depressions. The fault is filled with cataclastic surrounding sediments (mainly shales) with limited permeability.

Moderately (45–60°) mostly to the SE dipped NE–SW faults, are related with depression forming in the transtensional tectonic regime. The faults separate the depression basement into individual blocks. Tension tectonic has a positive impact on permeability and fluid flow. The same structure separates the northern Čížatice depression from the southern Ďurkov depression. Groundwater migration from the center of the basin towards the western edge at the contact with the Hornád fault system in the Košice area is likely occurring at these faults. As a result, disproportionally high groundwater temperatures are observed towards the western edge of the basin. Therefore, these are “key fault structures” that enabled the flow of overheated groundwater in the Košice Depression (Table 1).

**Table 1.** Basic fault parameters with different impacts on permeability and surface morphology.

Faults	Rank	Sense	Permeability	Morphology
NW-SE	I., III.	Inverse, shear, normal	closed	asymmetric
N-S	II.	shear, normal,	closed	horst/depressions
NE-SW	III., IV.	Normal	opened	-

Based on the results of the structural model in the southeastern part of Košice Depression, the so-called Ďurkov/Čížatice geothermal area, the thickness, and distribution of sedimentary packets, which are also considered as potential aquifers, has been modeled. The 3 D model is bounded on the east by the Sarmatian neovolcanic of Slanské vrchy Mts., which in places laterally extend into the filling of the sedimentary basin. The western



boundary of the model is represented by the N-S fault line, which is part of the Hornád fault zone. At these faults, the depth of the underlier reaches the greatest depths in the Košice Depression, which was verified by several wells. The Margecany shear zone borders the model from the south and the NE-SW fault from the north.

In the seismic profiles, five lithostratigraphic boundaries are interpreted. Seismic reflexes of the middle part of the profile indicate a pronounced pre-tertiary basement elevation, reflecting probably an uplift effect of the Sarmatian neovolcanites. Steeply dipped normal faults and/or oblique-slip faults detected within the profile reduce the Miocene sequences and markedly cut the Mesozoic formations. In the long axis of the model is possible to identify flexural bend separating Čizatice and Ďurkov structure. More information about the Miocene basement composition and deformation nature provide the KP-1, DUR-1, and DUR-2 wells. The last well penetrate heavily crushed Middle/Late Triassic dolomites [39]. Penetrating of the Late/Middle Triassic carbonates in the DUR-1 well ceased at 3200 m depth. The top section of the carbonates, which are underlying the Neogene successions, comprises light grey compact dolomite shales containing dynamo-metamorphic exsolutions of calcite veins. Dark grey clay/shale layers among dolomites appear, namely, at 2682–2753 m depth interval. From ca. 2750 m depth dolomites containing an increased  $\text{CaCO}_3$  (up to 45%) [40].

The modeling of evaluated seismic/well data allows specifying four lithostructural geothermal water aquifers (Figure 8) limited by the over/underlying bedding planes.

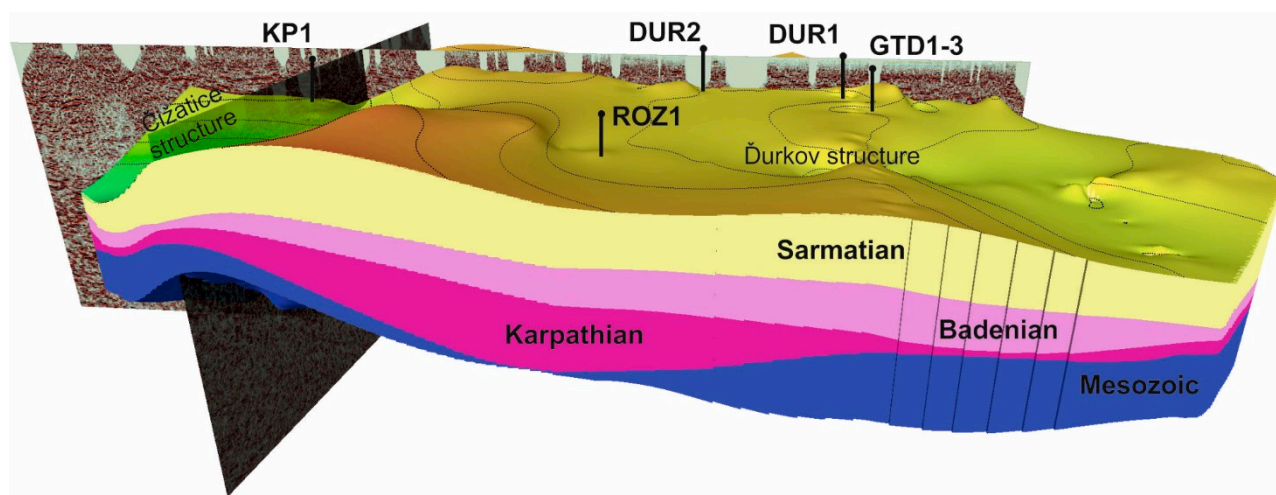


**Figure 8.** 3D geothermal model of the major lithological formations participated in the Košice Depression geological structure. The dolomites (blue) represent the main aquifer of the geothermal structure, which has an asymmetric shape in its N–S direction. In the model is a nice visible flexural boundary between Čizatice and Ďurkov structures (modified after [29]).

The first aquifer (AQ1) body forms the Mesozoic sequence of the Čierna hora Mts. Veporic unit. The deepest part of the Mesozoic pile, i. e. the basal aquifer plane (marked in violet color in Figure 8), reaches depth 2000 m to 2600 m, while a depth of its overlying pre-Neogene interface varies from 1250 m to 1380 m. The aquifer sole depth differences probably indicate topographical effects of pre-Neogene denudation and/or syn-postsedimentary tectonic processes. At the central part of the modeled section, an outstanding (blue-colored at Figure 9) elevation extends. The elevation separates the Ďurkov area depression of the SE edge of the section from the Čizatice graben structure developed at the western section margin. Both of the graben structures are reflecting probably NE-SW normal faulting. The Ďurkov graben structure is not as large as the previous surface, but the depression in the Čizatice area is still very outstanding. It is because of the increasing activity of the Miocene N-S or NE-SW faults. These two surfaces delimitate Triassic carbonate rocks, and variability in topography and thickness can be assumed. Only two wells from the plotted ones, i.e., KP-1 and ROZ-1, penetrate the Mesozoic pile sole. The overlying plane of the aquifer

elevation shows an uneven topography. Its deepest level reaches from 1800 m to ca. 2270 m, while the highest one from 800 m to 85 m only. Larger altitude differences, in comparison to the Mesozoic formations aquifer sole, seemingly reflect the post-Sarmatian fault activity and distinctly higher deformation competencies of overlying Neogene formations as well.

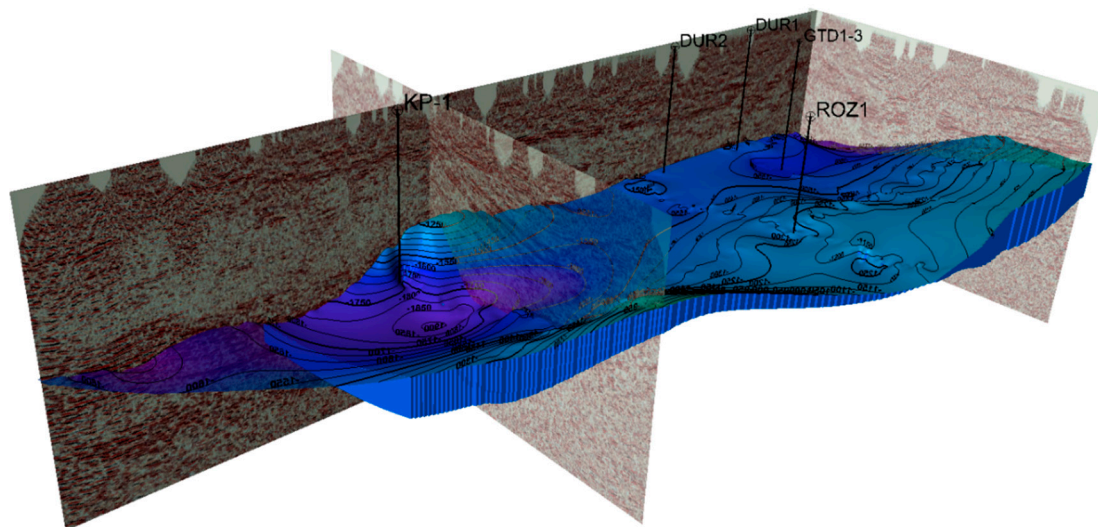


**Figure 9.** 3D model of the Middle Triassic buried dolomites under Košice depression. The thickness and inclination changes are influenced by fracture tectonics, which is an important structural phenomenon underlying the aquifer.

The second (AQ2) aquifer body form Karpathian clastic sediments (mainly conglomerates and sandstones). This Neogene basal formation lies directly on the Mesozoic aquifer, following in this manner topography of Mesozoic formations. The Karpathian deposits are conformably overlain by Lower/Middle Badenian fine-grained clastic sediments and evaporite sediments. The topography of this lithostratigraphic interface is not as rugged as in the previously discussed cases. The variation in depth shows ca. 260 ms (approx. 220 m). The surface deepest part reaches 1550 ms (ca. 1850 m), and the top-level reaches 600 ms (approx. 570 m). The intensity of N-S faults decreases, while NE-SW faults are still very outstanding.

The third (AQ3) aquifer body is sandwiched between the Lower/Middle Badenian and Upper Badenian boundaries. It has a moderate topography, but a distinct depression in the western part of the section surface achieves 1080 m amplitude. The maximal depth of the depression reaches ca. 1530 m, while its top point is located at ca. 450 m depth. Whereas, an activity of the NE-SW faults fades out in the depression, normal faulting at the NW-SE faults is still progressive.

The Upper Badenian/Sarmatian bedding plane terminates the fourth (AQ4) aquifer body. It forms the top surface of the model with a moderate topography of the boundary plane or its outstanding depression reaching ca. 910 m depth. The Sarmatian volcanoclastic sediments of the modeled area outcrops to the surface.

The following indicative/proportional volumetric calculation (the model comes out from 2D) of the individual lithostratigraphic horizons of the Košice depression forms one of the modeled outputs (Table 2). As it results from the cubature of the formations, the Karpathian aquifer possesses the highest capacity for geothermal water accumulations. Regarding volumetrically the second aquifer, it is necessary to mention, that only Mesozoic sequences comprising ca. 40.6 km<sup>3</sup> of calculated volume, could be effective for the discussed purposes. Such volumes are not present throughout the Košice depression. The thicknesses of dolomites in the Ďurkov/Čížatice area are many times thicker, which is related to their tectonic accumulation (duplexes) as a consequence of the uplift and unroofing of Čierna Hora Mts.

**Table 2.** Results of volumetric calculation of each modeled lithostratigraphic formation.

Body	Bulk Volume (km <sup>3</sup> )	Percentage (%)
Sarmatian	73,457	35.8
Badenian	34,674	16.9
Karpathian	56,285	27.5
Mesozoic	40,618	19.8

#### 4. Discussion

The creation of economically perspective geothermal water reservoirs at geological conditions of the East Slovakian basin (ESB) closely depends on a sufficient geothermal flow and a presence of compositionally/volumetrically adequate aquifers. Both are present in the western part of the ESB, especially the southeastern section of the Košice subbasin, more precisely in the Čižatice/Ďurkov structure.

Presented values reflect main rock formations data collected largely from the south-eastern margin of the Košice depression. They could be significantly influenced by initial compositional irregularities and the tectonic impact as well. The dolomitic aquifer (AQ1) of the Middle Triassic Period with underlying Verfenian shales,  $\pm$  quartzites, Permian cover formation, and crystalline basement rocks (as has been confirmed by mentioned KP-1 well) belongs to the Čierna hora Veporic unit [41]. The dolomitic complex shows the variable thickness and lateral development throughout the unit [42]. The thickness irregularities are related to duplexes of the Triassic dolomites observed in the surface and also in drill cores. At such conditions, a vertical duplication of the dolomitic sequences is multiplying their reservoir capacity. The thickness of the dolomite aquifer is variable. In the western edge at the contact with the basement, the Middle Triassic dolomite complex thickness is 185 m, towards to east it grows up to 1060 m.

The thickness of sedimentary layers is a key factor in terms of total groundwater reserves, but also for the calculation of the thermal gradient.

An average thermal gradient of the depression sedimentary fill varies from 36.5 to 50.3 °C/km or between 25.0–32.3 °C/km in pre-Tertiary rock formations, respectively [43]. The relatively high thermal gradient in the Neogene sequences relates to their lower thermal conductivity. The geothermal gradient generally increases towards the Pannonian basin (i.e., in the south direction), due to a substantially larger overheating of the thinning Earth crust. A tectonic brecciation and the hot water inflow at the faults are the other reasons for higher geothermal gradient raising within the Neogene sequences. At depths of 500–4000 m, i.e., at the depths of a presumable geothermal water aquifers location, the temperature ranges from 27–182 °C [44]. Thermal conductivity of particular lithotypes recorded regional and vertical characteristics of horizons. Thermal conductivity varies from 1.6 (W/mK) for coarse-grained formations and evaporites, 1.8 (W/mK) for fine-grained lithotypes, and 3.1 (W/mK) for carbonates in the Western Carpathians. The andesites observed in the SE part of the structure have defined thermal conductivity of 2.1 (W/mK). Hereby, mean geothermal values are used, and the possible impact of horizon thickness and depth of its top is limited to a minimum. Analysis of the sedimentary fill in the wells confirms a rather smaller thermal conductivity growth in the depth. While Sarmatian (AQ4) sediments show lower (i.e., 2.10 W/mK) thermal conductivity, the conductivity of Badenian and Karpatian (AQ3, AQ2) sediments is somewhat higher, i.e., 2.09 W/mK to 2.19 W/mK, respectively. The conductivity of Paleogene sandy/clay sediments shows a characteristic value of 2.31 W/mK. An average thermal conductivity of the Tertiary rocks varies about  $2.05 \pm 0.25$  W/mK (Table 3), while constant Mesozoic carbonate rocks display 3.62 W/mK [39]. The highest thermal flow values (i.e., 100–110 mW/m<sup>2</sup>) of the area have been detected at the foothills of the Slanské vrchy Mts. neovolcanic territory. In the central part of the Košice depression, typical values range between 85–95 mW/m<sup>2</sup>, while in its

western part, they vary at the 80–85 mW/m<sup>2</sup> interval. The average value of the Košice depression thermal flow reaches  $94.9 \pm 10.5$  mW/m<sup>2</sup>.

**Table 3.** Geothermal data summary.

Stratigraphy		Lithology	Thermal Gradient °C/km	Thermal Conductivity W/mK	
NEOGENE (23–2.5 Ma)	Sarmatian	claystones sandstones	38.1–51.4	2.10	av. 2.05 ± 0.25
	Badenian	claystones		2.10	
	Karpathian	conglomerates		2.19	
MESOZOIC (251–66 Ma)		dolomites limestones	22.4–30.6	3.62	

The groundwater geochemical analyzes from Košice depression show significant differences. Waters of the Ca-Mg-HCO<sub>3</sub> type with a hydrochemical coefficient Cl/Na = 0.75 predominate. These waters have origin in the dolomites of the Mesozoic unit of Čierna Hora Mts. The structure of Čižatice/Ďurkov is dominated by groundwater with NaCl content with a low proportion of Na-HCO<sub>3</sub>. From the origin point of view, these waters formed by the infiltration of probably meteoric/marine (subsequently marinogenic) water through Neogene formations (also salt marine sediments of Karpathian) into the Mesozoic collector [45,46]. By dissolving salts from salt formations, the waters contain small amounts of Br and have a Cl/Br ratio greater than 1000. It is a specific-polygenic type of geothermal water created when sea (marinogenic) water dissolves saline formations of the Karpathian. Their origin is probably in the area north of the Čižatice structure at the northern edge of the Košice Basin. The source may be in the evaporites of the Sol'ná Baňa Formation. The water solutions from them infiltrate through the NE-SW faults towards the south. On the contrary, their lateral distribution is limited by the sealing properties of the N-S Hornád fault system, and therefore, this type of water reaches the western edge of the basin.

The exploitation of geothermal energy in practice is primarily a source of possibilities. Even if a hyperthermal structure is missing slightly lower tempered geothermal water of this area is technologically utilizable for power generation and/or heating of Kosice town [39], as it is known from other world countries. For example, ORC binary power plants are designed for temperatures ranging from 45 °C (Alaska) to 225 °C (Hawaii) and are built in a variety of sizes [47–49]. For comparison, the Turkey government in 2015 build a low-temperature geothermal powerplant Tosunlar 1, with an output steam/brine of 105 °C and gross electrical generation of 3878 kW [50]. Residual heat can be used for secondary purposes, e.g., for tourism development, agricultural or industrial production.

## 5. Conclusions

Geothermal waters in the western edge of the East Slovakian basin saturate the Mesozoic karstified limestones and dolomites with fissure and karstic permeability.

- The thickness of the Mesozoic aquifer is increasing from the west (185 m) to the east (1060 m or more). The changes of thickness relate to the tectonic thickening of layers as a consequence of the uplift of the basement units on the western edge of the East Slovakian basin.
- The aquifer depth increase significantly from the west (0 m) to the east (2475 m) on a short distance of 20 km. The entire original horizon is subdivided into tectonic blocks with individual depth and lateral rate by the “domino” effect. The vertical subsidence of the tectonic blocks reaches 1200 m.
- The process of individualization of the tectonic blocks was successive. First, existing NW-SE and N-S pre-Miocene structures were preferred. Later, evolutionary younger dislocations and joints of NE-SW direction were active.



- The flow of the thermal groundwater in the fractures is closely linked to the dilatation structures of the NE-SW direction, which enabled the migration of waters from the basin center towards its western edge. The result is warm groundwater in wells (17 °C from depth 150 m, 26 °C from depth 300 m) at the western edge of the East Slovakian basin. Common temperatures are up to 9 °C.
- The geothermal structure contains three different chemical types of water confirmed by wells. Their spatial chemical distribution where Na-HCO<sub>3</sub> water type and 10.9 g·L<sup>-1</sup> mineralization (in the north), the Ca-Mg-HCO<sub>3</sub> with 0.5–4.5 g·L<sup>-1</sup> mineralization (in the west), and Na-Cl water type containing 20.4–33.1 g·L<sup>-1</sup> mineralization (in the southwest), correlate with open fissure distribution.
- Identifying critical tectonic structure is most important in the areas with a high tectonic impact on the geothermal aquifer. The future project for geothermal utilization of geothermal potential must implement all relevant datasets. The tectonics dataset is one of them.

**Author Contributions:** Conceptualization, S.J.; methodology, R.F.; validation, B.Š.; writing—original draft preparation, S.J.; writing—review and editing, K.B.; visualization, I.Ď. All authors have read and agreed to the published version of the manuscript.

**Funding:** This research was funded by the Slovak Grant Agency VEGA, grants. 1/0585/20.” and by the GeoSurvey company grant No. 10/501501/19 and 3/501501/20.

**Institutional Review Board Statement:** Not applicable.

**Informed Consent Statement:** Informed consent was obtained from all subjects involved in the study.

**Conflicts of Interest:** The authors declare no conflict of interest.

## References

1. Allansdottir, A.; Pellizzone, A.; Sciullo, A. Geothermal Energy and Public Engagement. In *Geothermal Energy and Society. Lecture Notes in Energy*; Manzella, A., Allansdottir, A., Pellizzone, A., Eds.; Springer: Cham, Switzerland, 2019; Volume 67, pp. 55–65. [\[CrossRef\]](#)
2. Lund, J.W.; Toth, A.N. Direct utilization of geothermal energy 2020 worldwide review. *Geothermics* **2021**, *90*, 101915. [\[CrossRef\]](#)
3. Lund, J.W.; Boyd, T.J. Direct utilization of geothermal energy 2015 worldwide review. *Geothermics* **2016**, *60*, 66–93. [\[CrossRef\]](#)
4. Lund, J.W.; Freeston, D.H.; Boyd, T.J. Direct utilization of geothermal energy 2010 worldwide review. *Geothermics* **2011**, *40*, 159–180. [\[CrossRef\]](#)
5. Lund, J.W.; Freeston, D.H.; Boyd, T.J. Direct applications of geothermal energy 2005 worldwide review. *Geothermics* **2006**, *34*, 691–727. [\[CrossRef\]](#)
6. Lund, J.W.; Freeston, D.H. World-wide direct uses of geothermal energy 2000. *Geothermics* **2001**, *30*, 29–68. [\[CrossRef\]](#)
7. Lund, J.W.; Toth, A.N. Direct utilization of geothermal energy 2020 worldwide review. In *Proceedings of the World Geothermal Congress 2020, Reykjavik, Iceland, 26 April–2 May 2020*.
8. Erlingsson, T.; Thorhallsson, S. Long Distance Transmission Pipelines for Geothermal Waters in Iceland (20–60 km). In *Proceedings of the Workshop for Decision Makers on Direct Heating Use of Geothermal Resources in Asia*, organized by UNU-GTP, TBLRREM and TBGMED, Tianjin, China, 11–18 May 2008.
9. Horváth, F.; Musitz, B.; Balázs, A.; Véghe, A.; Uhrine, A.; Nádor, A.; Koroknai, B.; Pap, N.; Tótha, T.; Wórum, G. Evolution of the Pannonian basin and its geothermal resources. *Geothermics* **2015**, *53*, 328–352. [\[CrossRef\]](#)
10. Dövényi, P.; Horváth, F. A review of temperature, thermal conductivity, and heat flow data from the pannonian basin. In *The Pannonian Basin: A Study in Basin Evolution*; Royden, L.H., Horváth, F., Eds.; AAPG Memoir 45; American Association of Petroleum Geologists: Tulsa, OK, USA, 1988; Volume 45, pp. 195–235.
11. Dövényi, P.; Horváth, F.; Drahos, D. Geothermal thermic map (Hungary). In *Atlas of Geothermal Resources in Europe*; Hurter, S., Haenel, R., Eds.; 267. Publication No. EUR 17811; Office for Official Publications of the European Communities: Luxembourg, 2002; 267p.
12. Horváth, F.; Sztanó, O.; Uhrin, A.; Fodor, L.; Balázs, A.; Kóbor, M.; Wórum, G. Towards a dynamic model for the formation of the Pannonian basin. In *Proceedings of the EGU General Assembly 2012, Vienna, Austria, 22–27 April 2012*; Geophysical Research Abstracts. Volume 14.
13. Franko, O.; Fendek, M.; Remšík, A. *Geothermal Energy of the Slovak Republic*; Štátny Geologický Ústav Dionýza Štúra: Bratislava, Slovakia, 1995; 90p.
14. Kováč, M.; Bielik, M.; Hók, J.; Kováč, P.; Kronone, B.; Labák, P.; Moczo, P.; Plašienka, D.; Šefara, J.; Šujan, M. Seismic activity and neotectonic evolution of the Western Carpathians (Slovakia). *EGU Stephan Mueller Spec. Publ. Ser.* **2002**, *3*, 167–184. [\[CrossRef\]](#)

15. Tari, G.; Dövényi, P.; Dunkl, I.; Horváth, F.; Lenkey, L.; Stefanescu, M.; Szafian, P.; Tóth, T. Lithospheric structure of the Pannonian basin derived from seismic, gravity and geothermal data. *Geol. Soc. Lond. Spec. Publ.* **1999**, *156*, 215–250. [\[CrossRef\]](#)
16. Jarosinski, M.; Beekman, F.; Matenco, L.; Cloetingh, S. Mechanics of basin inversion: Finite element modelling of the Pannonian Basin System. *Tectonophysics* **2011**, *502*, 196–220. [\[CrossRef\]](#)
17. Lenkey, L.; Dövényi, P.; Horváth, F.; Cloetingh, S.A.P.L. Geothermics of the Pannonian basin and its bearing on the neotectonics. *EGU Stephan Mueller Spec. Publ. Ser.* **2002**, *3*, 29–40. [\[CrossRef\]](#)
18. Ustaszewski, K.; Kounov, A.; Schmid, S.M.; Schaltegger, U.; Krenn, E.; Frank, W.; Fügenschuh, B. Evolution of the Adria-Europe plate boundary in the northern Dinarides: From continent-continent collision to back-arc extension. *Tectonics* **2010**, *29*, TC6017. [\[CrossRef\]](#)
19. Ustaszewski, K.; Schmid, S.M.; Fügenschuh, B.; Tischler, M.; Kissling, E.; Spakman, W. A map-view restoration of the Alpine-Carpathian-Dinaridic system for the Early Miocene. *Swiss J. Geosci.* **2008**, *101* (Suppl. 1), 273–294. [\[CrossRef\]](#)
20. Kováč, M.; Kováč, P.; Marko, F.; Karoli, S.; Janočko, J. The East Slovakian Basin—A complex back-arc basin. *Tectonophysics* **1995**, *252*, 453–466. [\[CrossRef\]](#)
21. Fričovský, B.; Černák, R.; Marcin, D.; Blanárová, V.; Benková, K.; Pelech, O.; Fordinál, K.; Bodiš, D.; Fendek, M. Geothermal energy use—country update for Slovakia. In Proceedings of the World Geothermal Congress 2020, Reykjavik, Iceland, 26 April–1 May 2020.
22. Kaličiak, M.; Baňacký, V.; Janočko, J.; Karoli, S.; Petro, L.; Spišák, Z.; Vozár, J.; Žec, B. *Geological Map of the Slánske vrchy Mts. and Košice Depression—South part M 1: 50,000*; Lib. of the Slovak Geol. Survey: Bratislava, Slovakia, 1996.
23. Pachocka, K.; Jacko, S.; Pachocki, M. *3D modeling of a Geothermal Reservoir in Eastern Slovakia Area: The Central Part of Kosice Basin*; VDM Verl.: Saarbrücken, Germany, 2010; 62p.
24. Beardsmore, G.R.; Cull, J.P. *Thermal Conductivity In Crustal Heat Flow: A Guide to Measurement and Modelling*; Beardsmore, G.R., Cull, J.P., Eds.; Cambridge University Press: New York, NY, USA, 2001; pp. 90–145. [\[CrossRef\]](#)
25. Čverčko, J. *Final Report from Pioneer Borehole Ďurkov-2*; Manuscript; Lib. of the Slovak Geol. Survey: Bratislava, Slovakia, 1970; pp. 1–98.
26. Čverčko, J.; Magyar, J.; Rudinec, R.; Jung, F.; Lunga, S.; Očovský, J.; Varga, M.; Mořkovský, M.; Lukášová, R. *Final Report from Deep Research Well in the East Slovakian Basin*; Manuscript; Lib. of the Slovak Geol. Survey: Bratislava, Slovakia, 1983; pp. 1–135.
27. Rudinec, R. *Sources of Oil, Gas and Geothermal Energy in the Eastern Slovakia*; Alfa Lib.: Bratislava, Slovakia, 1989; pp. 1–162.
28. Pereszlenyi, M.; Pereszlenyiova, A.; Masaryk, P. Geological setting of the Košice Basin in relation to geothermal energy resources. *Bulletin d'Hydrogeologie* **1999**, *17*, 115–122.
29. Jacko, S.; Labant, S.; Bátorová, K.; Farkašovský, R.; Ščerbáková, B. Structural constraints of neotectonic activity in the eastern part of the Western Carpathians orogenic wedge. *Quat. Int.* **2020**. [\[CrossRef\]](#)
30. Jacko, S. New Upper Triassic Formations in Mesozoic of the Čierna Hora Mts. *Geol. Práce* **1987**, *Správy 87*, 19–25.
31. Jacko, S.; Farkašovský, R.; Kondela, J.; Mikus, T.; Scerbakova, B.; Dirnerova, D. Boudinage arrangement tracking of hydrothermal veins in the shear zone: Example from the argenteiferous Strieborna vein (Western Carpathians). *J. Geosci.* **2019**, *64*, 179–195. [\[CrossRef\]](#)
32. Čverčko, J. The Faults of the East Slovakian Basin and Their Tectogenetic Evolution. Ph.D. Thesis, Geofond, Bratislava, Slovakia, 1977; pp. 1–143. Available online: <https://www.geology.sk/sluzby/digitalny-archiv/> (accessed on 20 February 2021).
33. Vass, D. *The Fault System Evaluation in Košice Depression with Special View to Tahanovce and Krasna n. Hornadom Area. Final Report of Slovak Geological Survey*; Geofond: Bratislava, Slovakia, 1979; 18p. Available online: <https://www.geology.sk/sluzby/digitalny-archiv/> (accessed on 20 February 2021).
34. Kaličiak, M.; Baňacký, V.; Janočko, J.; Karoli, S.; Petro, L.; Spišák, Z.; Vozár, J.; Žec, B. *Explanation to Geological map of the Slánske Mts. and Kosice Depression—Southeastern*; Slovak Geological Survey: Bratislava, Slovakia, 1996; pp. 1–206.
35. Jacko, S.; Janočko, J.; Jacko, S. Tectonic evolution of the southern part of the Central-Carpathian Paleogene Basin in the Eastern Slovakia. *Geol. Carpathica* **2002**, *53*, 155–156.
36. Kováč, M.; Márton, E.; Oszczypko, N.; Vojtko, R.; Hók, J.; Králiková, S.; Plašienka, D.; Klučiar, T.; Hudáčková, N.; Oszczypko-Clowes, M. Neogene palaeogeography and basin evolution of the Western Carpathians, Northern Pannonian domain and adjoining areas. *Glob. Planet. Chang.* **2017**, *155*, 133–154. [\[CrossRef\]](#)
37. Márton, E.; Vass, D.; Túnyi, I. Counterclockwise rotations of the Neogene rocks in the East Slovak Basin. *Geol. Carpathica* **2000**, *51*, 159–168.
38. Jacko, S.; Farkašovský, R.; Dirnerová, D.; Kondela, J.; Rzepa, G.; Zákršmidová, B. The Late Cretaceous conditions of the Gom-515 basak beds sedimentation (Silica nappe, Western Carpathians). *Acta Montan. Slovaca* **2016**, *21*, 259–271.
39. Jacko, S.; Fričovský, B.; Pachocká, K.; Vranovská, A. Stationary reverse temperature modeling and geothermal resources calibration for the Košice depression (Eastern Slovakia). *Technika poszukiwań geologicznych: Geotermia, Zrównowazony rozwój* **2014**, *53*, 3–25.
40. Fričovský, B.; Jacko, S.; Popovičová, M.; Tometz, L. Substitution Approach in Carbon Dioxide Emission Reduction Evaluation: Case Study on Geothermal Power Station Project Plan-Ďurkov (Košice Basin, Slovakia). *Int. J. Environ. Sci. Dev.* **2013**, *4*, 124–129. [\[CrossRef\]](#)
41. Rudinec, R. *Interaction between Sedimentary Fill and Pro-Neogene Basement in Central Part of the Košice-Prešov Depression*; Nafta Michalovce Lib.: Michalovce, Slovakia, 1973; pp. 1–75.

- 
42. Král, M.; Lizoň, I.; Jančí, J. *Geothermic Research in Slovakia. Final Report from 1981 to 1985*; Lib. of the Slovak Geol. Survey: Bratislava, Slovakia, 1985; 116p.
  43. Vizi, L.; Fričovský, B.; Zlocha, M.; Surový, M. Use of Geostatistical Simulation in Reservoir Thermodynamics Assessment and Interpretation at the Ďurkov Hydrogeothermal Structure, Slovakia. *Slovak Geol. Mag.* **2020**, *20*, 85–98.
  44. Fričovský, B.; Jacko, S.; Chytilová, M.; Tometz, L. Geothermal energy of Slovakia-CO<sub>2</sub> emissions reduction contribution potential (background study for conservative and non-conservative approach). *Acta Montan. Slovaca* **2012**, *17*, 290–299.
  45. Bodiš, D.; Vranovská, A. Genesis of anomalous arsenic content in the hydrogeothermal structure of Ďurkov. *Podzemná voda* **2012**, *XVIII*, 123–136.
  46. Vranovská, A. *Košice Depression—Ďurkov Structure—Hydrogeothermal Evaluation*; Final Report; Ministry of Environment of the Slovak Republic: Bratislava, Slovakia, 1999; 79p.
  47. Bronicki, L.Y. Organic Rankine Cycles in Geothermal Power Plants: 25 Years of Ormat Experience. *GRC Trans.* **2007**, *31*, 499–502.
  48. Quoilin, S.; Broek, M.V.D.; Declaye, S.; Dewallef, P.; Lemort, V. Techno-Economic Survey of Organic Rankine Cycle (ORC) Systems. *Renew. Sustain. Energy* **2013**, *22*, 168–186. [[CrossRef](#)]
  49. Tontu, M.; Sahin, B.; Bilgili, M. An exergoeconomic–environmental analysis of an organic Rankine cycle system integrated with a 660 MW steam power plant in terms of waste heat power generation. *Energy Sources Part A Recovery Util. Environ. Eff.* **2020**, 1–22. [[CrossRef](#)]
  50. Mertoglu, O.; Simsek, S.; Basarir, N.; Paksoy, H. Geothermal Energy Use, Country Update for Turkey. In Proceedings of the European Geothermal Congress, Den Haag, The Netherlands, 11–14 June 2019.